Am J Transl Res 2017;9(11):5074-5093
www.ajtr.org /ISSN:1943-8141/AJTR0055857

Original Article

Extracorporeal shock wave therapy effectively protects brain against chronic cerebral hypo-perfusion-induced neuropathological changes

Han-Tan Chai[1*], Kuan-Hung Chen[2*], Christopher Glenn Wallace[3], Chih-Hung Chen[4], Pei-Hsun Sung[1], Yung-Lung Chen[1], Chun-Man Yuen[5], Pei-Lin Shao[6], Cheuk-Kwan Sun[7], Hsueh-Wen Chang[8], Ching-Jen Wang[9,10], Mel S Lee[9], Hon-Kan Yip[1,6,10,11,12], Sheung-Fat Ko[13]

[1]Division of Cardiology, Department of Internal Medicine, Kaohsiung Chang Gung Memorial Hospital and Chang Gung University College of Medicine, Kaohsiung 83301, Taiwan; [2]Department of Anesthesiology, Kaohsiung Chang Gung Memorial Hospital and Chang Gung University College of Medicine, Kaohsiung 83301, Taiwan; [3]Department of Plastic Surgery, University Hospital of South Manchester, Manchester, UK; [4]Divisions of General Medicine, Department of Internal Medicine, Kaohsiung Chang Gung Memorial Hospital and Chang Gung University College of Medicine, Kaohsiung 83301, Taiwan; [5]Division of Neurosurgery, Department of Surgery, Kaohsiung Chang Gung Memorial Hospital and Chang Gung University College of Medicine, Kaohsiung 83301, Taiwan; [6]Department of Nursing, Asia University, Taichung, 41354, Taiwan; [7]Department of Emergency Medicine, E-DA Hospital, I-Shou University, Kaohsiung 82445, Taiwan; [8]Department of Biological Sciences, National Sun Yat-sen University, Kaohsiung, 80424, Taiwan; [9]Department of Orthopedics, Kaohsiung Chang Gung Memorial Hospital and Chang Gung University College of Medicine, Kaohsiung 83301, Taiwan; [10]Center for Shockwave Medicine and Tissue Engineering, Kaohsiung Chang Gung Memorial Hospital and Chang Gung University College of Medicine, Kaohsiung 83301, Taiwan; [11]Institute for Translational Research in Biomedical Sciences, Kaohsiung Chang Gung Memorial Hospital, Kaohsiung 83301, Taiwan; [12]Department of Medical Research, China Medical University Hospital, China Medical University, Taichung, 40402, Taiwan; [13]Department of Radiology, Kaohsiung Chang Gung Memorial Hospital and Chang Gung University College of Medicine, Kaohsiung 83301, Taiwan. [*]Equal contributors.

Received April 20, 2017; Accepted July 22, 2017; Epub November 15, 2017; Published November 30, 2017

Abstract: This study tested the hypothesis that extracorporeal shock wave (ECSW) therapy could protect mouse brain from chronic cerebral hypoperfusion (CHP)-induced neuropathological changes in a bilateral carotid arterial stenosis (CAS) model. Adult-male C57BL/6 (B6) mice (n=36) were randomized into group 1 (sham-control), group 2 (CHP) and group 3 [CHP+ECSW (100 impulses at 0.15 mJ/mm^2) on day 5, 10 and 15 after CHP induction]. By day 60 after CHP induction, the white matter lesion, protein expressions of inflammatory (TNF-α/NF-κB/iNOS), oxidative-stress (NOX-1/NOX-2/NOX-4/nitrotyrosine), angiogenesis (eNOS/CD31), apoptotic (Bax/caspase-3/PARP), fibrotic (Smad3/TGF-ß) and mitochondrial-damaged (cytosolic cytochrome-C) biomarkers were significantly higher in group 2 than in groups 1 and 3, and significantly higher in group 3 than in group 1, whereas the protein expressions of anti-apoptotic (Bcl-2), anti-fibrotic (BMP-2/Smad1/5), and mitochondrial-integrity (mitochondrial cytochrome-C) biomarkers showed an opposite pattern to inflammation among the three groups (all P<0.0001). The cellular expressions of inflammatory (Iba-1/GFAP/CD14, F4/80), apoptotic (TUNEL-assay) and brain-damaged (γ-H2AX/AQP4) biomarkers showed an identical pattern to inflammation, whereas the cellular expressions of endothelial-cell (CD31/vWF), neuron/energy-integrity (NeuN/PGC-1α) and small-vessel density exhibited an opposite pattern to inflammation among the three groups (all P<0.0001). Cellular angiogenesis (VEGF/SDF-1α) significantly and progressively increased from groups 1 to 3 (all P<0.0001). In conclusion, ECSW therapy enhanced angiogenesis, inhibited molecular-cellular perturbations, and protected the white matter and neuron from CHP damage.

Keywords: Chronic cerebral hypoperfusion, inflammation, apoptosis, oxidative stress, angiogenesis, extracorporeal shock wave therapy

Introduction

Dementia represents a syndrome of acquired intellectual deficits resulting in significant impairment of social and occupational function and is increasingly an economic burden worldwide [1-4]. The possible etiologies for dementia are diverse [5], but ischemic cerebrovascular

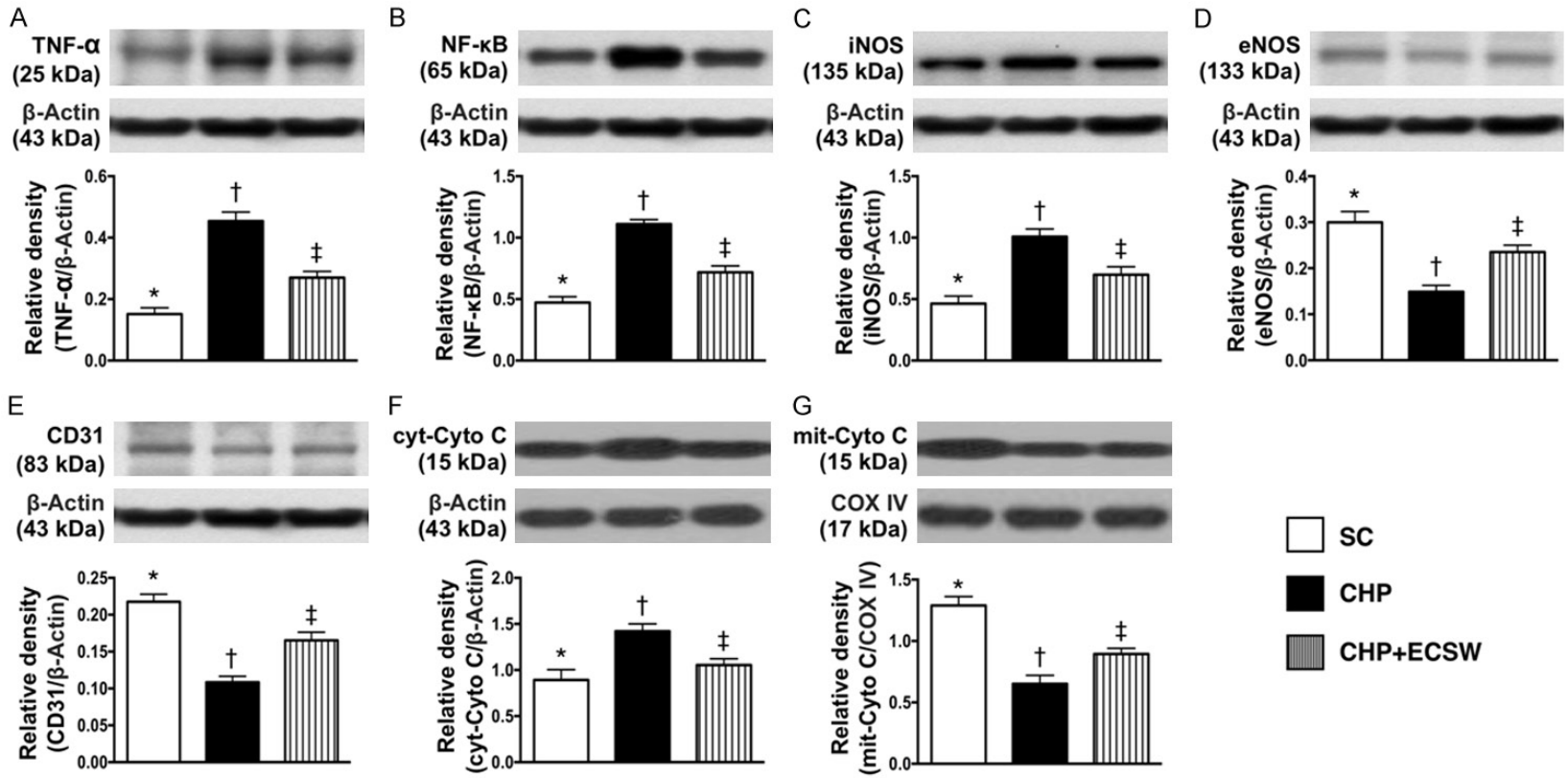

Figure 1. Protein expressions of inflammatory, endothelial and cytochrome C biomarkers at day 60 after CHP induction. A. Protein expression of tumor necrosis factor (TNF)-α, * vs. other groups with different symbols (†, ‡), P<0.001. B. Protein expression of nuclear factor (NF)-κB, * vs. other groups with different symbols (†, ‡), P<0.001. C. Protein expression of inducible nitric oxide synthase (iNOS), * vs. other groups with different symbols (†, ‡), P<0.001. D. Protein expression of endothelial nitric oxide synthase (eNOS), * vs. other groups with different symbols (†, ‡), P<0.001. E. Protein expression of CD31, * vs. other groups with different symbols (†, ‡), P<0.001. F. Protein cytosolic cytochrome C (cyt-Cyto C), * vs. other groups with different symbols (†, ‡), P<0.003. G. Protein expression of mitochondrial cytochrome C (mit-Cyto C), * vs. other groups with different symbols (†, ‡), P<0.001. All statistical analyses were performed by one-way ANOVA, followed by Bonferroni multiple comparison post hoc test (n=6 for each group). Symbols (*, †, ‡, §) indicate significance (at 0.05 level). SC = sham control; CHP = chronic cerebral hypoperfusion; ECSW = extracorporeal shock wave.

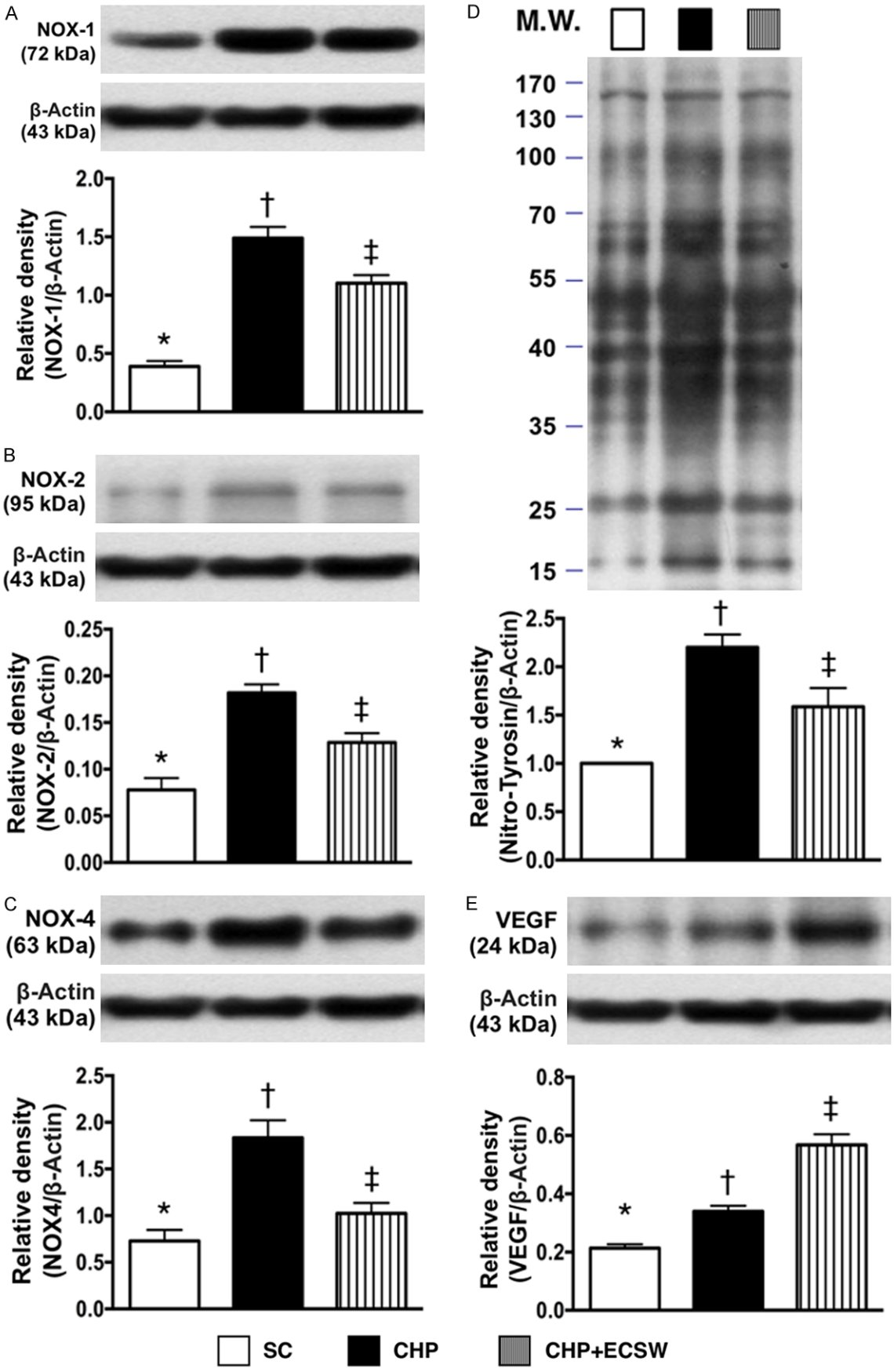
A
NOX-1
(72 kDa)
β-Actin
(43 kDa)
Relative density
(NOX-1/β-Actin)
2.0
1.5
1.0
0.5
0.0
*
†
‡
B
NOX-2
(95 kDa)
β-Actin
(43 kDa)
Relative density
(NOX-2/β-Actin)
0.25
0.20
0.15
0.10
0.05
0.00
C
NOX-4
(63 kDa)
β-Actin
(43 kDa)
Relative density
(NOX4/β-Actin)
2.5
2.0
1.5
1.0
0.5
0.0
D
M.W.
170
130
100
70
55
40
35
25
15
Relative density
(Nitro-Tyrosin/β-Actin)
E
VEGF
(24 kDa)
β-Actin
(43 kDa)
Relative density
(VEGF/β-Actin)
0.8
0.6
0.4
0.2
0.0
SC
CHP
CHP+ECSW

Figure 2. Protein expressions of oxidative stress and angiogenesis biomarkers at day 60 after CHP induction. A. Protein expression of NOX-1, * vs. other groups with different symbols (†, ‡), P<0.001. B. Protein expression of NOX-2, * vs. other groups with different symbols (†, ‡), P<0.001. C. Protein expression of NOX-4, * vs. other groups with different symbols (†, ‡), P<0.001. D. Protein expression of nitrotyrosine, * vs. other groups with different symbols (†, ‡), P<0.01. M.W. = molecular weight. E. Protein expression of vascular endothelial growth factor (VEGF), * vs. other groups with different symbols (†, ‡), P<0.0001. All statistical analyses were performed by one-way ANOVA, followed by Bonferroni multiple comparison post hoc test (n=6 for each group). Symbols (*, †, ‡, §) indicate significance (at 0.05 level). SC = sham control; CHP = chronic cerebral hypoperfusion; ECSW = extracorporeal shock wave.

disease (CVD) is considered a major cause especially in the elderly. The spectrum of vascular cognitive impairments caused by various types of CVD occur due to interactions between a variety of vascular risk factors such as hypertension, obesity, dyslipidemia, diabetes mellitus, chronic ischemic stroke (IS) and silent IS [6-8].

Age-related chronic cerebral hypoperfusion (CHP) is commonly caused by carotid artery stenosis and atherosclerotic arterial occlusive diseases of larger and small intracranial vessels, which result from various etiologies that lead, subsequently, to ischemic white matter lesions (WML) [6, 8] and later dementia. Despite pharmacological advances and carotid artery stenosis interventions, an effective treatment for CHP-related dementia is still lacking [1, 5, 8].

Compared with other organs, the brain is more susceptible to damage from oxidative-stress due to its high metabolic rate, high polyunsaturated lipid content, and lower levels of endogenous antioxidant activity and self-protection mechanisms. WML caused by chronic CHP may play an essential role in the development of vascular-impaired dementia (VID) via the upregulation of oxidative stress and inflammation [9-14]. Thus, a therapeutic modality for dementia in chronic CHP patients could involve abrogating oxidative stress and inflammation as well as restoration of blood flow through enhancing angiogenesis in the hypoperfused brain.

Extracorporeal shock wave (ECSW) therapy is well known for providing a mechanical means of treatment, such as lithotripsy for kidney and urethral stones. Its low-energy form (ranging from 0.03 to 0.15 mJ/mm^2) can also elicit a series of subtle biological effects for treating the musculoskeletal [15, 16] and cardiovascular systems [17-20]. Studies have also shown that ECSW therapy improves ischemia-related organ dysfunction by suppressing the inflammatory response and the generation of reactive oxygen species (ROS), and by enhancing angiogenesis/neovascularization [17-21]. However, whether ECSW can effectively reverse CHP-induced WM lesions and VID has not been investigated. Accordingly, the present study used a mouse chronic CHP model (i.e., induction of bilateral carotid arterial stenosis using micro-coils) to test the hypothesis that ECSW therapy could effectively inhibit chronic CHP-induced brain damage.

Materials and methods

Ethics

All animal experimental protocols and procedures were approved by the Institute of Animal Care and Use Committee at Kaohsiung Chang Gung Memorial Hospital (Affidavit of Approval of Animal Use Protocol No. 2015062302) and performed in accordance with the Guide for the Care and Use of Laboratory Animals [The Eighth Edition of the Guide for the Care and Use of Laboratory Animals (NRC 2011)].

Animals were housed in an Association for Assessment and Accreditation of Laboratory Animal Care International (AAALAC)-approved animal facility in our hospital (IACUC protocol no. 101008) with controlled temperature and light cycles (24°C and 12/12 light cycles).

Experimental protocol and animal grouping

The experimental protocol was based on our previous report with minimal modification [4]. Twelve-week old male C57Bl/6J mice (n=36) weighing 25-30 g (Charles River Technology, BioLASCO Taiwan Co. Ltd., Taiwan) were categorized into sham control (SC, n=12), CHP (induced by bilateral carotid artery stenosis procedure, n=12], and CHP + ECSW [(100 impulses at 0.15 mJ/mm^2) on day 5, 10 and 15 after CHP induction, n=12].

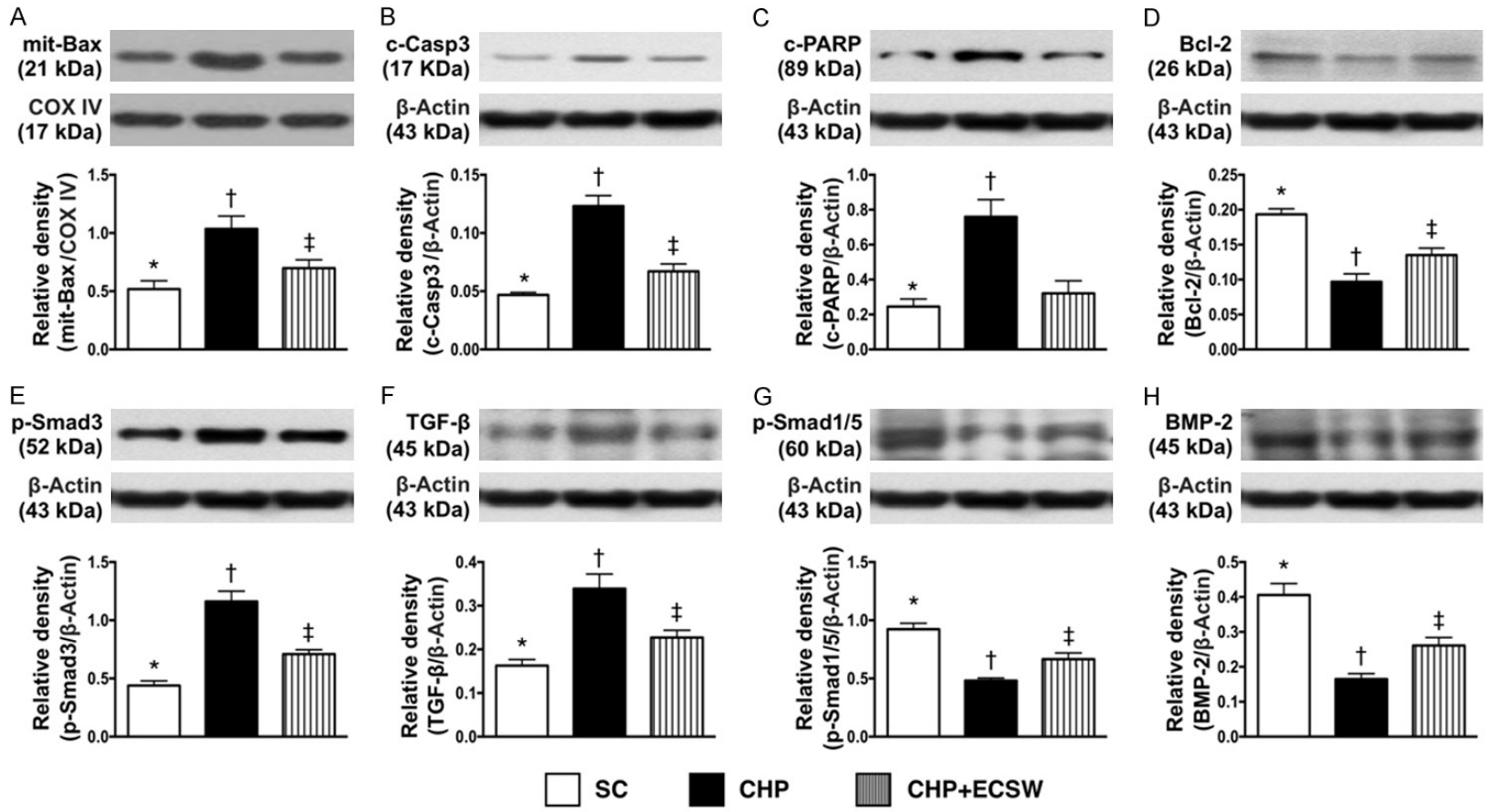

Figure 3. Protein expressions of apoptotic, anti-apoptotic, fibrotic and antifibrotic biomarkers at day 60 after CHP induction. A. Protein expression of mitochondrial Bax, * vs. other groups with different symbols (†, ‡), P<0.001. B. Protein expression of cleaved caspase 3, (c-Casp3), * vs. other groups with different symbols (†, ‡), P<0.001. C. Protein expression of cleaved Poly (ADP-ribose) polymerase (c-PARP), * vs. other groups with different symbols (†, ‡), P<0.001. D. Protein expression of Bcl-2, * vs. other groups with different symbols (†, ‡), P<0.001. E. Protein expression of Phospho-Smad3, * vs. other groups with different symbols (†, ‡), P<0.001. F. Protein expression of transforming growth factor-ß, * vs. other groups with different symbols (†, ‡), P<0.001. G. Protein expressions of Phospho-Smad1/5, * vs. other groups with different symbols (†, ‡), P<0.001. H. Protein expression of bone morphogenetic protein (BMP)-2, * vs. other groups with different symbols (†, ‡), P<0.001. All statistical analyses were performed by one-way ANOVA, followed by Bonferroni multiple comparison post hoc test (n=6). Symbols (*, †, ‡) indicate significance (at 0.05 level). SC = sham control; CHP = chronic cerebral hypoperfusion; ECSW = extracorporeal shock wave.

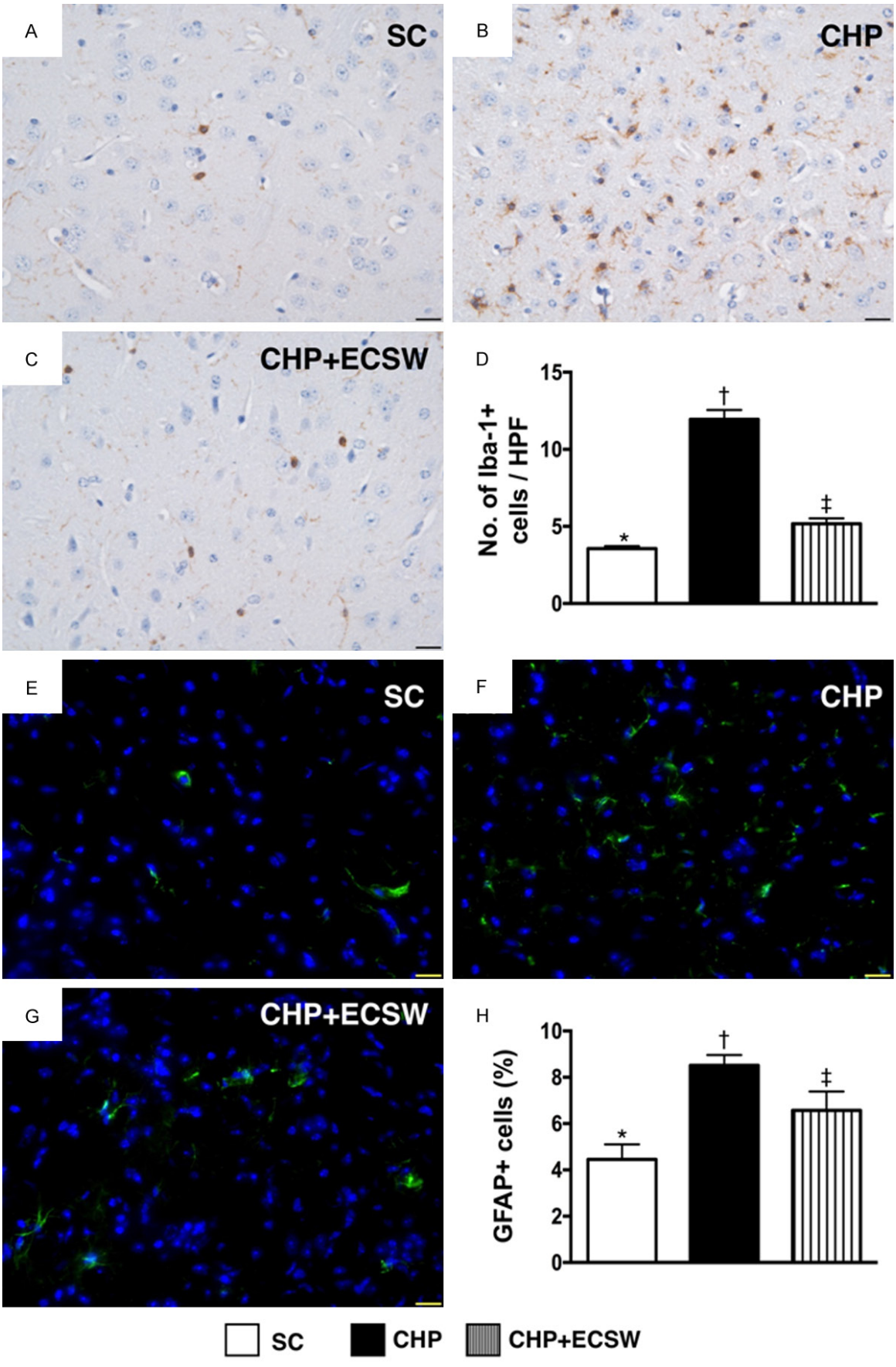
A
SC
B
CHP
C
CHP+ECSW
D
No. of Iba-1+ cells / HPF
15
10
5
0
*
†
‡
E
SC
F
CHP
G
CHP+ECSW
H
GFAP+ cells (%)
10
8
6
4
2
0
*
†
‡
SC
CHP
CHP+ECSW

Figure 4. Cellular expression of inflammation in brain tissue at day 60 after CHP induction. A-C. Illustrating microscopy findings (400×) using immunohistochemical staining to identify Iba-1+ cells (gray). D. Analytical results of number of positively-stained Iba-1 cells, * vs. other groups with different symbols (†, ‡), P<0.001. E-G. Illustrating microscopy findings (400×) of immunofluorescent staining to identify glial fibrillary acid protein (GFAP)+ cells (green). H. Analytical results of number of positively-stained GFAP cells, * vs. other groups with different symbols (†, ‡), P<0.001. Scale bars at the right lower corner represent 20 μm. All statistical analyses were performed by one-way ANOVA, followed by Bonferroni multiple comparison post hoc test (n=6). Symbols (*, †, ‡) indicate significance (at 0.05 level). SC = sham control; CHP = chronic cerebral hypoperfusion; ECSW = extracorporeal shock wave.

Bilateral carotid artery constriction

The protocol and procedure were based on our previous report [4]. All animals were anesthetized (inhalational 2.0% isoflurane) and placed supine on a warming pad at 37°C during the BCAS procedure. Both sides of the neck were incised and the carotid arteries identified. Bilateral carotid artery stenoses were induced by encasing both common carotid arteries within micro-coils (Sawane Spring Co, Shizuoka, Japan; internal diameter 0.18 mm) to cause luminal narrowing. Sham-control mice received an identical operation without micro-coil placement on the carotid arteries.

Specimen collection and preparation for individual study

The procedure and protocol for specimen collection have previously been reported [4, 19, 22-24]. For examination of protein expression, animals in all groups were sacrificed on day 60 after brain acute IS procedure, and the brain of each rat was promptly removed, immersed in cold saline, snap-frozen in liquid nitrogen and then stored at -80°C for individual study. For immunofluorescent (IF) and immunohistochemical (IHC) staining studies, the brains of 6 other animals in each group were reperfused with normal saline via the carotid artery, removed, fixed with 4% paraformaldehyde in 1× PBS (pH 7.4), and soaked in 20% sucrose in 1× PBS (freshly prepared) until the brain took on a completely sunken appearance. The sucrose was then discarded and the brain soaked in 30% sucrose in 1× PBS (freshly prepared) for 48 h; the tissue specimen was then retrieved. Finally, an OCT block (Tissue-Tek, Sakura, Netherlands) was prepared for IHC and IF staining.

Histopathology scoring, and immunohistochemical (IHC) and immunofluorescent (IF) staining

Kluver-Barrera staining was used to determine the WM lesions. We counted the number of vacuolation of neurons in internal capsule/corpus callosum (i.e., WM lesions) of cortex in 4 animals from each group.

The procedure and protocol of IF and IHC were based on our previous reports [4, 19, 22-24]. In detail, frozen sections (4 μm thick) were obtained from BIA of each animal, permeated with 0.5% Triton X-100, and incubated with antibodies against NeuN (1:1000, Millipore, Billerica, MA, USA), glial fibrillary acid protein (GFAP; 1:500, DAKO, Carpinteria, CA, USA), aquaporin4 (AQP4; 1:200, Abcam, Cambridge, MA, USA), Iba-1 (1:500; wako, Chuo-ku, Osaka, Japan), CD14 (1:200, Bioss, Massachusetts, Boston, USA), F4/80 (1:100; Abcam, Cambridge, MA, USA), γ-H2AX (1:1000; Abcam, Cambridge, MA, USA), vascular endothelial cell growth factor (VEGF) (1:400; Abcam, Cambridge, MA, USA), peroxisome proliferator-activated receptor gamma coactivator 1-alpha (PGC-1α) (1:100; Novus, Oakville, Ontario, Canada), stromal cell-derived factor (SDF)-1α (1:100, Santa Cruz Biotechnology), white matter lesion (WML) (i.e., Kluver-Barrera staining), TUNEL assay (In Situ Cell Death Detection Kit POD, Roche, Basel, Switzerland), α-SMA (1:400, Sigma-Aldrich, St. Louis, Missouri, USA), and von Willebrand Factor (vWF) (1:200, Millipore, Massachusetts, USA) at 4°C overnight. Alexa Fluor488, Alexa Fluor568, or Alexa Fluor594-conjugated goat anti-mouse or rabbit IgG were used to localize signals. Sections were finally counterstained with DAPI and observed with a fluorescent microscope equipped with epifluorescence (Olympus IX-40).

Three brain sections were analyzed for each mouse. For quantification, three randomly selected high-power fields (HPFs; ×400 for IHC and IF studies) were analyzed in each section. The mean number of positively-stained cells per HPF for each animal was then determined by summation of all numbers divided by 9.

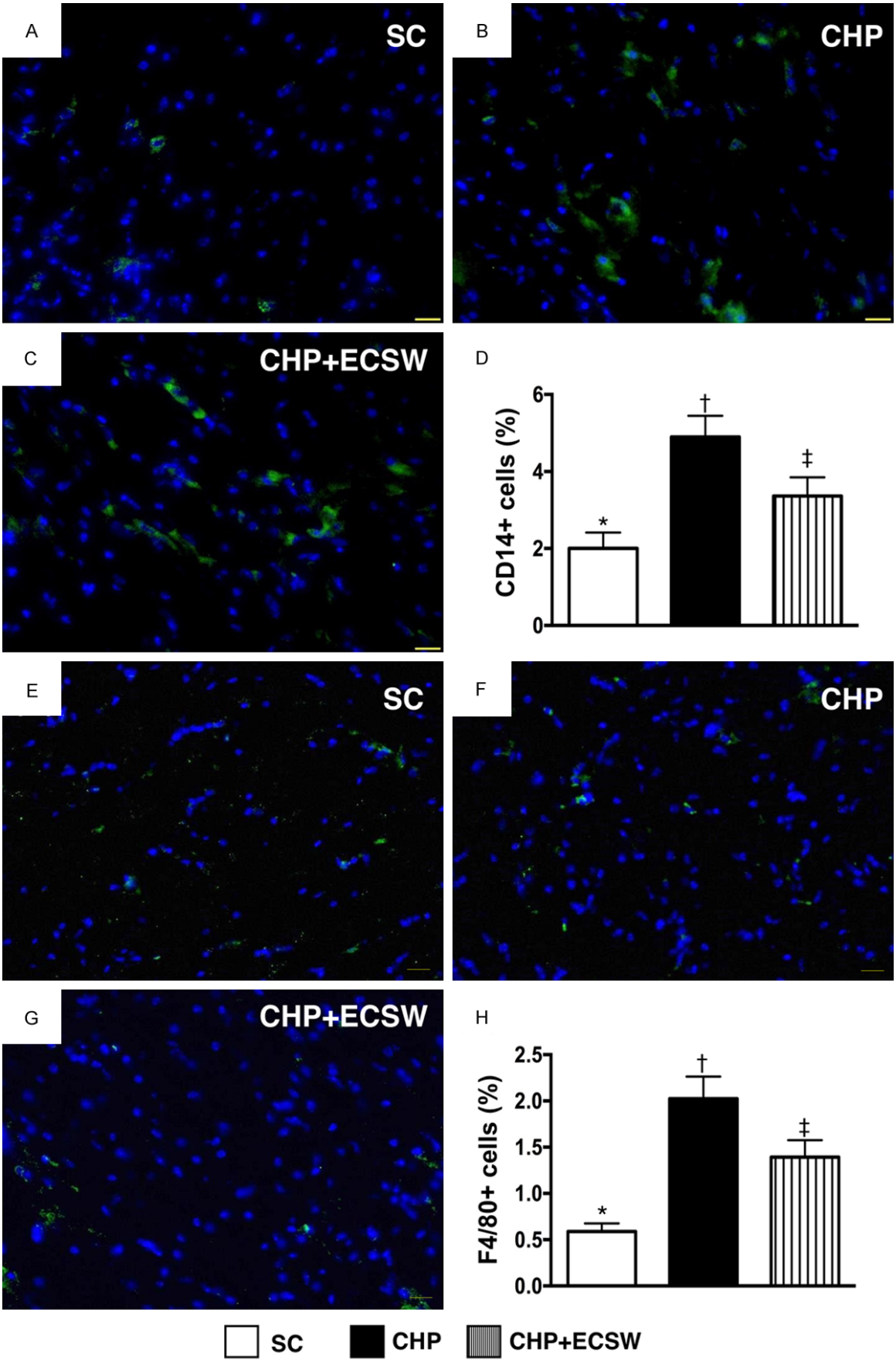
A
SC
B
CHP
C
CHP+ECSW
D
CD14+ cells (%)
6
4
2
0
*
†
‡
E
SC
F
CHP
G
CHP+ECSW
H
F4/80+ cells (%)
2.5
2.0
1.5
1.0
0.5
0.0
*
†
‡
SC
CHP
CHP+ECSW

Figure 5. Cellular innate immune response in brain tissue at day 60 after CHP induction. A-C. Illustrating microscopy findings (400×) using immunofluorescent (IF) staining to identify CD14+ cells (green). D. Analytical results of number of positively-stained CD14 cells, * vs. other groups with different symbols (†, ‡), P<0.001. E-G. Illustrating microscopy findings (400×) of immunofluorescent staining to identify F4/80+ cells (green). H. Analytical results of number of positively-stained F4/80 cells, * vs. other groups with different symbols (†, ‡), P<0.001. Scale bars in the right lower corner represent 20 μm. All statistical analyses were performed by one-way ANOVA, followed by Bonferroni multiple comparison post hoc test (n=6). Symbols (*, †, ‡) indicate significance (at 0.05 level). SC = sham control; CHP = chronic cerebral hypoperfusion; ECSW = extracorporeal shock wave.

Western blot analysis of brain specimens

The procedure and protocol of Western blot were based on our previous reports [4, 22-24]. Equal amounts (50 μg) of protein extracts were loaded and separated by SDS-PAGE using 12% acrylamide gradients. After electrophoresis, the separated proteins were transferred electrophoretically to a polyvinylidene difluoride (PVDF) membrane (Amersham Biosciences, Amersham, UK). Nonspecific sites were blocked by incubation of the membrane in blocking buffer [5% nonfat dry milk in T-TBS (TBS containing 0.05% Tween 20)] overnight. The membranes were incubated with monoclonal antibodies against NOX-1 (1:1500, Sigma-Aldrich), NOX-2 (1:1000, Sigma-Aldrich), NOX-4 (1:1000, Abcam), nitrotyrosin (1:1000, Abcam), tumor necrosis factor alpha (TNF-α) (1:1000, Cell Signaling), nuclear factor (NF)-κB (1:1000, Abcam), inducible nitric oxide synthase (iNOS) (1:200, Abcam), Cytochrome C (1:2000, BD Bioscience, San Jose, CA, USA), Aquaporin 4 (1:750, Abcam), nuclear factor (NF)-κB (1:1000, Abcam), endothelial nitric oxide synthase (eNOS) (1:1000, Abcam), CD31 (1:1000, Abcam), Bax (1:1000, Abcam), Caspase 3 (1:1000, Cell Signaling), Poly (ADP-ribose) polymerase (PARP) (1:1000, Cell Signaling), Bcl-2 (1:600, Abacm), cytosolic cytochrome C (1:1000, BD), mitochondrial cytochrome C (1:1000, BD), phosphorylated (p)-Smad3, p-Smad1/5, transforming growth factor (TGF)-ß (1:5000, Abcam), and bone morphogenetic protein (BMP)-2 (1:500, Abcam) for 1 hr at room temperature. Horseradish peroxidase-conjugated anti-rabbit or anti-mouse immunoglobulin IgG (1:2000, Cell Signaling) was used as a second antibody for 1 hr at room temperature. The washing procedure was repeated eight times within 1 h, and immunoreactive bands were visualized by enhanced chemiluminescence (ECL; Amersham Biosciences) and exposure to Medical X-ray film (FUJI). For quantification, ECL signals were digitized using Labwork software (UVP, Waltham, MA, USA). A standard control sample was loaded on each gel.

TUNEL assay for apoptotic nuclei

For each rat, six sections of BIA were analyzed with an in situ Cell Death Detection Kit, AP (Roche) according to the manufacturer's guidelines. Three randomly chosen high-power fields (HPFs) (×400) were observed for terminal deoxynucleotidyltransferase-mediated 2'-deoxyuridine 5'-triphosphate nick-end labeling (TUNEL)-positive cells for each section. The mean number of apoptotic nuclei per HPF for each animal was obtained by dividing the total number of cells by 18.

Assessment of oxidative stress

The procedure and protocol for evaluating the protein expression of oxidative stress have previously been described [4, 22-24]. The Oxyblot Oxidized Protein Detection Kit was purchased from Chemicon, Billerica, MA, USA (S7150). DNPH derivatization was carried out on 6 μg of protein for 15 minutes according to the manufacturer's instructions. One-dimensional electrophoresis was carried out on 12% SDS/polyacrylamide gel after DNPH derivatization. Proteins were transferred to nitrocellulose membranes that were then incubated in the primary antibody solution (anti-DNP 1:150) for 2 hours, followed by incubation in secondary antibody solution (1:300) for 1 hour at room temperature. The washing procedure was repeated eight times within 40 minutes. Immunoreactive bands were visualized by enhanced chemiluminescence (ECL; Amersham Biosciences, Amersham, UK) and then exposed to Biomax L film (Kodak, Rochester, NY, USA). For quantification, ECL signals were digitized using Labwork software (UVP, Waltham, MA, USA). For oxyblot protein analysis, a standard control was loaded on each gel.

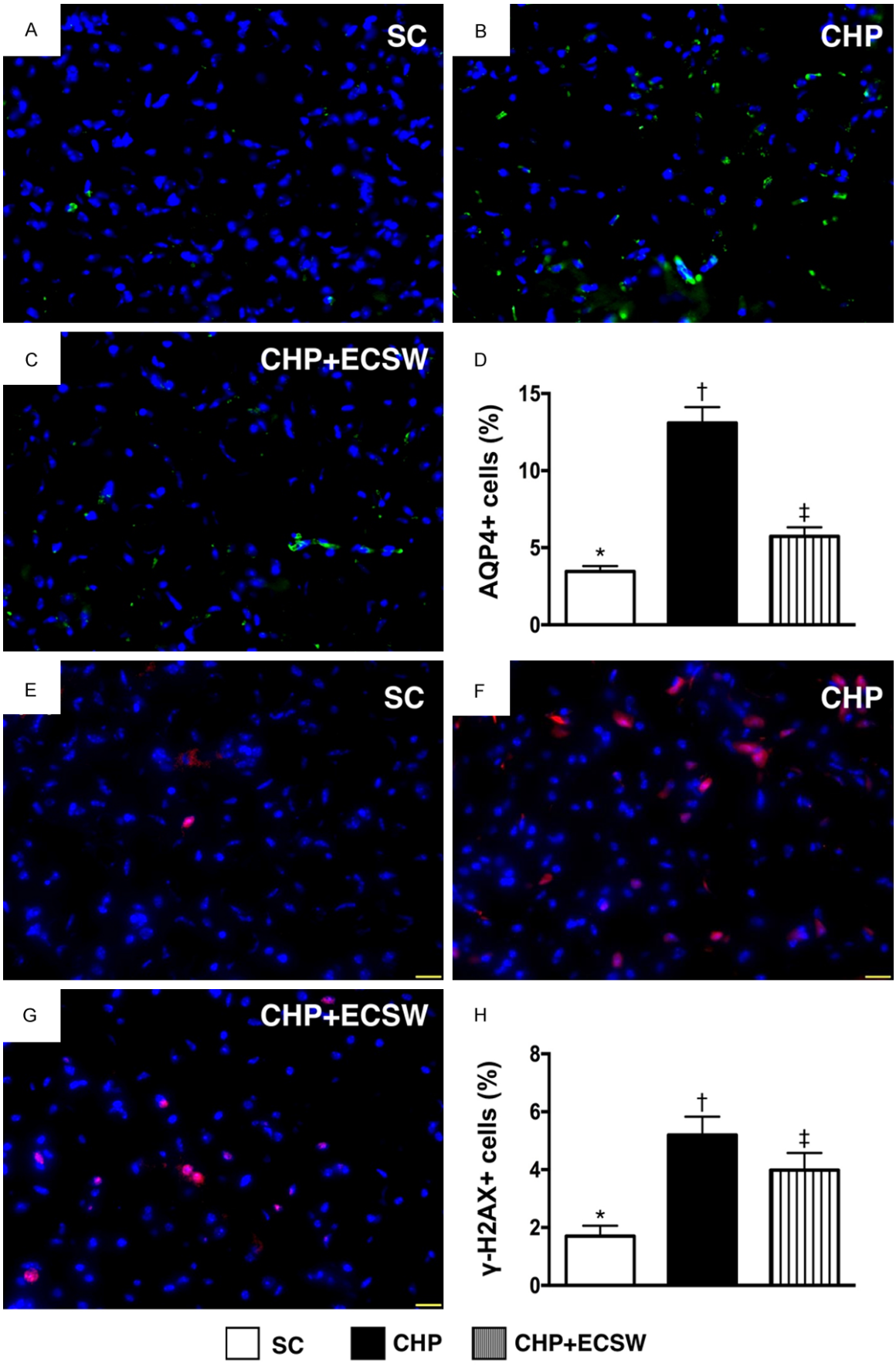
A
SC
B
CHP
C
CHP+ECSW
D
AQP4+ cells (%)
15
10
5
0
*
†
‡
E
SC
F
CHP
G
CHP+ECSW
H
γ-H2AX+ cells (%)
8
6
4
2
0
*
†
‡
SC
CHP
CHP+ECSW

Figure 6. Cellular expressions of brain edema and DNA-damage biomarkers in brain tissue at day 60 after CHP induction. A-C. Illustrating microscopy findings (400×) using immunofluorescent (IF) staining to identify aquaporin 4 (AQP4)+ cells (green). D. Analytic result of number of positively-stained AQP4 cells, * vs. other groups with different symbols (†, ‡), P<0.0001. E-G. Illustrating microscopy findings (400×) of immunofluorescent staining to identify γ-H2AX+ cells (green). H. Analytic result of number of positively-stained γ-H2AX cells, * vs. other groups with different symbols (†, ‡), P<0.001. Scale bars in the right lower corner represent 20 μm. All statistical analyses were performed by one-way ANOVA, followed by Bonferroni multiple comparison post hoc test (n=6). Symbols (*, †, ‡) indicate significance (at 0.05 level). SC = sham control; CHP = chronic cerebral hypoperfusion; ECSW = extracorporeal shock wave.

Statistical analyses

Quantitative data are expressed as mean ± SD. Statistical analysis was performed by ANOVA followed by Bonferroni multiple-comparison *post hoc* test. All analyses were conducted using SAS statistical software for Windows version 8.2 (SAS institute, Cary, NC). A probability value <0.05 was considered statistically significant.

Results

*The protein expressions of inflammatory, endothelial and cytochrome C biomarkers at day 60 after CHP induction (**Figure 1**)*

The protein expressions of TNF-α, NF-κB, and iNOS, three indicators of inflammation, were significantly higher in CHP than in SC and CHP-ECSW, and significantly higher in CHP-ECSW than in SC. Protein expressions of eNOS and CD31, two indicators of endothelial-integrity, showed an opposite pattern to inflammation among the three groups.

The protein expression of cytosolic cytochrome C, an indicator of mitochondrial damage was significantly higher in CHP than in SC and CHP-ECSW, and significantly higher in CHP-ECSW than in SC. Protein expression of mitochondrial cytochrome C, an indicator of mitochondrial integrity, showed an opposite pattern to cytosolic cytochrome C among the three groups.

*Protein expressions of oxidative stress and angiogenesis markers at day 60 after CHP induction (**Figure 2**)*

The protein expressions of NOX-1, NOX-2, NOX-4 and nitrotyrosine, four indicators of oxidative stress, were significantly higher in CHP than in SC and CPH-ECSW, significantly higher in CHP-ECSW than in SC and CHP-ECSW, and significantly higher in CHP-ECSW than in SC. Protein expression of VEGF, an indicator of angiogenesis, significantly increased from SC to CHP-ECSW, suggesting that an increase in VEGF was an intrinsic response to ischemic stimulation and further enhanced by ECSW therapy.

*Protein expressions of apoptotic, anti-apoptotic, fibrotic and antifibrotic biomarkers at day 60 after CHP induction (**Figure 3**)*

The protein expressions of mitochondrial Bax, cleaved caspase 3 and cleaved PARP, three indicators of apoptosis, were significantly higher in CHP than in SC and CHP-ECSW, and significantly higher in CHP-ECSW than in SC. Protein expression of Bcl-2, an indicator for anti-apoptosis, exhibited an opposite pattern to apoptosis among the three groups.

The protein expressions of Phospho-Smad3 and TGF-ß, two indicators of fibrosis, were significantly higher in CHP than in SC and CHP-ECSW, and significantly higher in CHP-ECSW than in SC, whereas, the protein expressions of Phospho-Smad1/5 and BMP-2, two indicators of anti-fibrosis, displayed an opposite pattern to fibrosis among the three groups.

*The cellular expressions of inflammation at day 60 after CHP induction (**Figure 4**)*

The cellular expressions of Iba-1 and GFAP, two inflammation indicators in brain parenchyma, were significantly higher in CHP than in SC and CHP-ECSW, and significantly higher in CHP-ECSW than in SC.

*The cellular innate immune response at day 60 after CHP induction (**Figure 5**)*

Microscopy demonstrated that the cellular expressions of CD14 and F4/80, two cellular indicators of innate immunity, were significantly

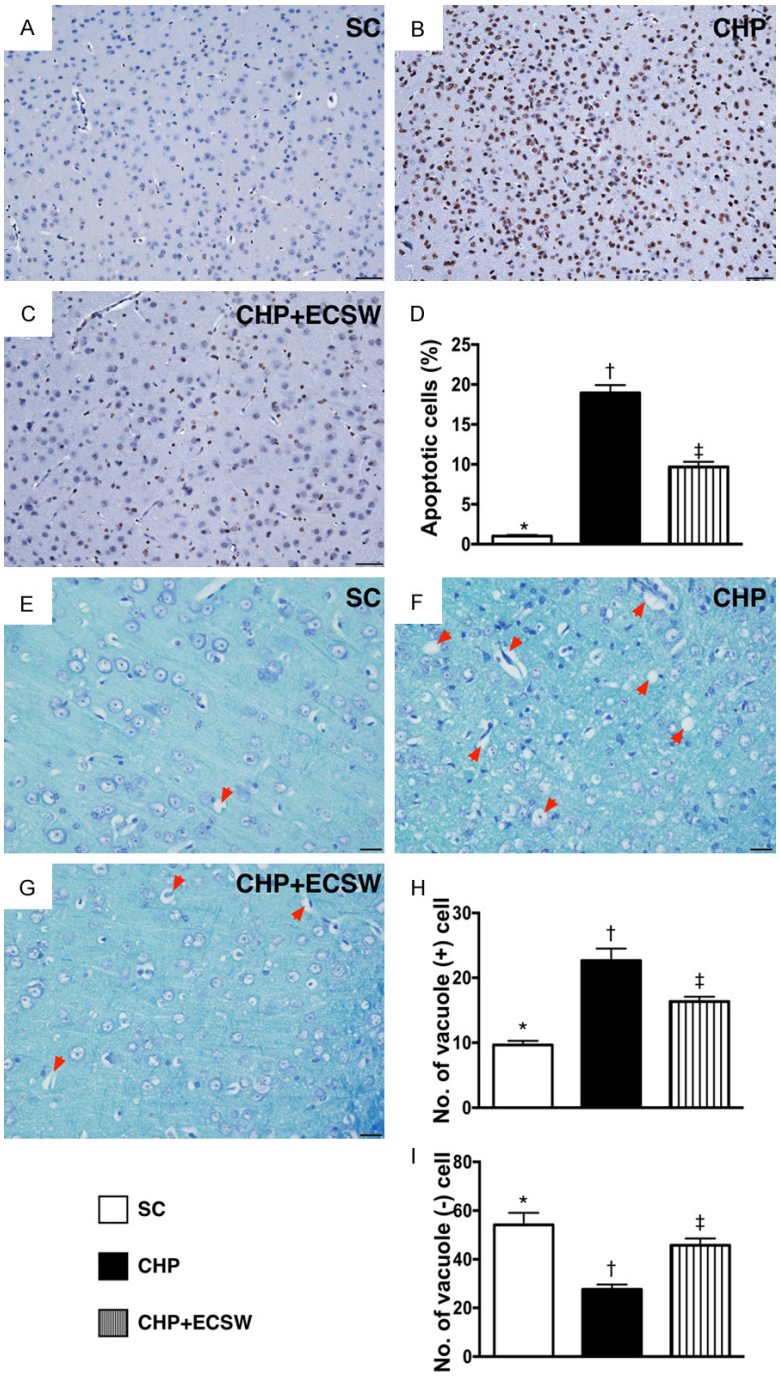

Figure 7. The cellular expressions of apoptosis and white matter lesion in brain tissue at day 60 after CHP induction. A-C. Illustrating the TUNEL assay (400×) for identification of apoptotic nuclei (gray). D. Analytical result of number of apoptotic nuclei, * vs. other groups with different symbols (†, ‡), P<0.0001. E-G. Illustrating microscopy findings (400×) using immunohistochemical staining to identify the vacuole neuron in white matter area (red). H. Statistically analytical results of number of vacuole neurons; * vs. other groups with different symbols (†, ‡), P<0.0001. I. Statistically analytical results of number of normal architectural neurons; * vs. other groups with different symbols (†, ‡), P<0.0001.Scale bars in the right lower corner represent 20 μm. All statistical analyses were performed by one-way ANOVA, followed by Bonferroni multiple comparison post hoc test (n=6). Symbols (*, †, ‡) indicate significance (at 0.05 level). SC = sham control; CHP = chronic cerebral hypoperfusion; ECSW = extracorporeal shock wave.

higher in CHP than in SC and CHP-ECSW, and significantly higher in CHP-ECSW than in SC.

*The cellular expressions of apoptotic and DNA-damage biomarkers at day 60 after CHP induction (**Figure 6**)*

IF microscopy showed that the number of AQP4+ cells, a biomarker for brain edema, was significantly higher in CHP than in SC and CHP-ECSW, and significantly higher in CHP-ECSW than in SC. Additionally, IF microscopy showed that the cellular expression of γ-H2AX, a biomarker for DNA-damage, exhibited an identical pattern to apoptotic nuclei.

*The cellular expressions of apoptosis and white matter lesion at day 60 after CHP induction (**Figure 7**)*

TUNEL assay showed that the number of apoptotic nuclei was significantly higher in CHP than in SC and CHP-ECSW and significantly higher in CHP-ECSW than in SC. Additionally, the number of vacuole neurons in WM, an indicator for WML, displayed an identical pattern to apoptotic nuclei among the three groups. On the other hand, the number of normal architectural neurons (i.e., normal neurons) exhibited an opposite pattern of apoptosis among the three groups.

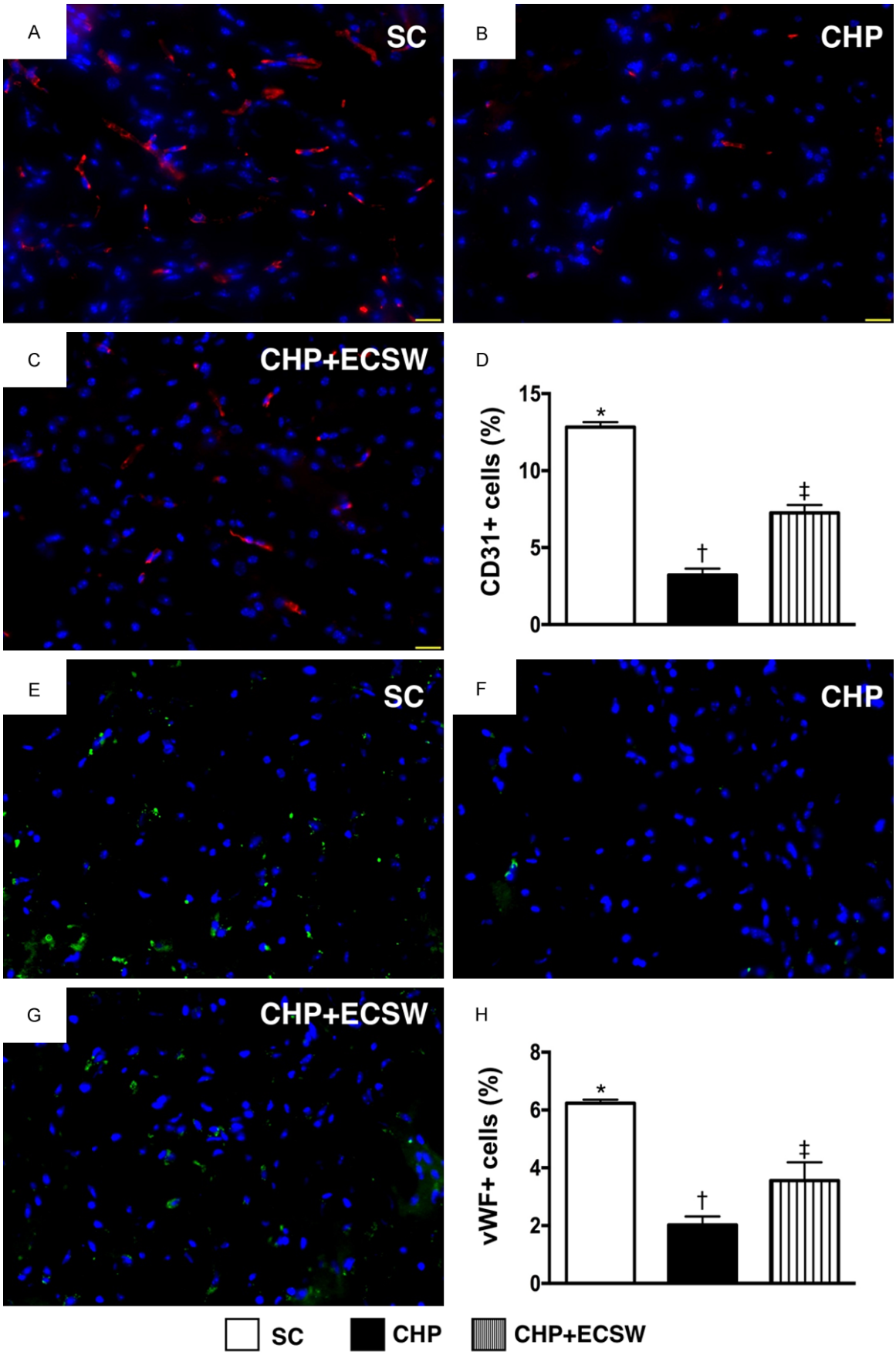
A
SC
B
CHP
C
CHP+ECSW
D
CD31+ cells (%)
15
10
5
0
*
†
‡
E
SC
F
CHP
G
CHP+ECSW
H
vWF+ cells (%)
8
6
4
2
0
*
†
‡
SC
CHP
CHP+ECSW

Figure 8. Cellular expression of endothelial cell biomarkers in brain tissue at day 60 after CHP induction. A-C. Illustrating microscopy findings (400×) using immunofluorescent (IF) staining to identify CD31+ cells (red). D. Analytical result of number of positively-stained CD31 cells, * vs. other groups with different symbols (†, ‡), P<0.0001. E-G. Illustrating microscopy findings (400×) using immunofluorescent (IF) staining to identify von Willebrand Factor (vWF)+ cells (green). H. Analytical result of number of positively-stained vWF cells, * vs. other groups with different symbols (†, ‡), P<0.0001. Scale bars in the right lower corner represent 20 μm. All statistical analyses were performed by one-way ANOVA, followed by Bonferroni multiple comparison post hoc test (n=6). Symbols (*, †, ‡) indicate significance (at 0.05 level). SC = sham control; CHP = chronic cerebral hypoperfusion; ECSW = extracorporeal shock wave.

*The cellular expressions of angiogenesis biomarkers at day 60 after CHP induction (**Figures 8** and **9**)*

IF microscopy for cellular expressions of CD31 and vWF, two endothelial cell biomarkers, were significantly higher in SC than in CHP and CHP-ECSW, and significantly higher in CHP-ECSW than in HCP (**Figure 8**).

Microscopy for cellular expressions of VEGF and SDF-1α, two indicators of angiogenesis, were significantly increased from SC to CHP-ECSW (**Figure 9**).

*The cellular expressions of neuron and energy integrity biomarkers at day 60 after CHP induction (**Figure 10**)*

IF microscopy showed that the cellular expression of NeuN, indicating neuron integrity, was significantly higher in SC than in CHP and CHP-ECSW, and significantly higher in CHP-ECSW than in CHP. Cellular expression of PGC-1α, an indicator of energy preservation, and number of small vessels, an indicator for angiogenesis/neovascularization, exhibited an identical pattern to neuN among the three groups.

*Small vessel (≤25 μM) density in brain tissue at day 60 after CHP induction (**Figure 11**)*

IHC microscopy showed that the number of the small vessels, an indicator of angiogenesis/neovascularization in cerebral tissue, was significantly higher in SC than in CHP and CHP-ECSW, and significantly higher in CHP-ECSW than in CHP.

Discussion

This study investigated the impact of ECSW treatment on protecting the brain against chronic CHP damage and yielded several striking implications. First, as compared with the SC group, WML was significantly increased in the CHP group and yet was notably reduced in CHP animals after receiving ECSW treatment. Second, compared with SC animals, the integrity of neuN cells was disrupted in CHP animals and yet preserved in CHP-ECSW animals. Third, angiogenesis capacity was attenuated in the CHP group compare to the SC group, but this was significantly reversed in the CHP-ECSW group. The intensities of inflammation and oxidative stress were markedly enhanced in CHP animals than in SC animals, but this was markedly ameliorated in CHP-ECSW animals.

It is well known that WML plays an important role in the initiation and propagation of dementia. Additionally, copious studies have established that CVD is a major contributor for ischemia-related WML and dementia [6, 8]. The most important finding in the present study was that WML was notably higher in chronic CHP animals compared to SC animals. Our experimental study, therefore, supports clinical observational studies [6, 8], highlighting that bilateral carotid artery stenosis (a scenario of CHP/ischemia) commonly causes WML. Importantly, ECSW therapy protected WM against chronic CHP damage, suggesting that ECSW therapy may have great potential for dementia patients who are refractory or failing to respond to conventional therapies.

An essential finding in the present study was that the number of neuN cells (neurons) was significantly reduced in CHP animals than SC animals. This demonstrates that CHP damaged the myelin sheath as well as the neuron in brain. Our previous study also showed that the number of neuN cells was markedly reduced in rats after acute ischemic stroke, and this was ameliorated with ECSW therapy [19]. In the present study, we identified that ECSW therapy significantly protected the number and integrity of neuN cells. The present study therefore corroborates our previous findings [19].

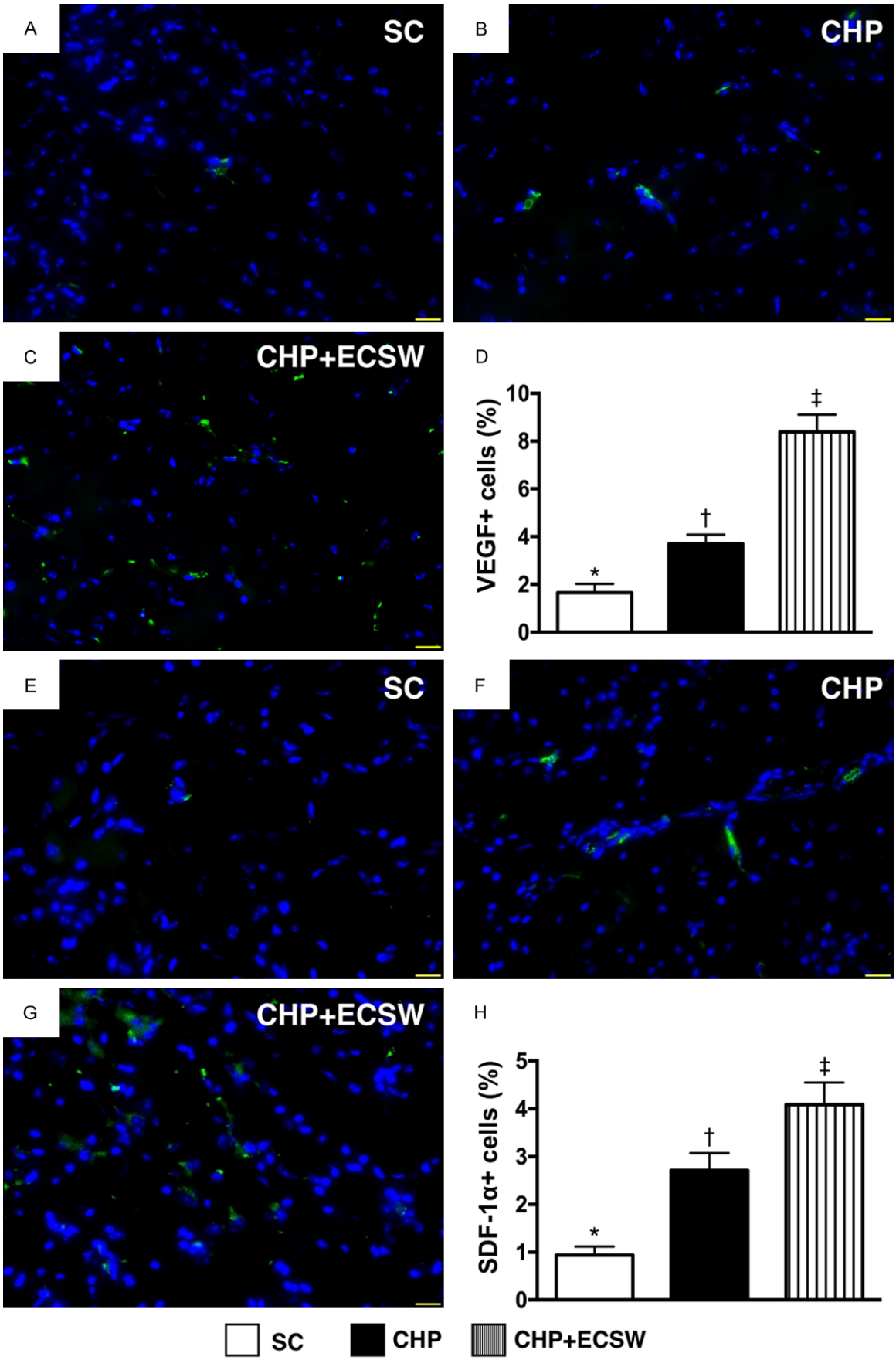
A
SC
B
CHP
C
CHP+ECSW
D
VEGF+ cells (%)
10
8
6
4
2
0
*
†
‡
E
SC
F
CHP
G
CHP+ECSW
H
SDF-1α+ cells (%)
5
4
3
2
1
0
*
†
‡
SC
CHP
CHP+ECSW

Figure 9. Cellular expressions of angiogenesis biomarkers in brain tissueat day 60 after CHP induction. A-C. Illustrating microscopy findings (400×) using immunofluorescent (IF) staining to identify vascular endothelial growth factor (VEGF)+ cells (green). D. Analytical result of number of positively-stained VEGF cells, * vs. other groups with different symbols (†, ‡), P<0.001. E-G. Illustrating microscopy findings (400×) using immunofluorescent (IF) staining to identify stromal cell-derived factor (SDF)-1α+ cells (green). H. Analytical result of number of positively-stained SDF-1α cells, * vs. other groups with different symbols (†, ‡), P<0.0001. Scale bars in the right lower corner represent 20 μm. All statistical analyses were performed by one-way ANOVA, followed by Bonferroni multiple comparison post hoc test (n=6). Symbols (*, †, ‡) indicate significance (at 0.05 level). SC = sham control; CHP = chronic cerebral hypoperfusion; ECSW = extracorporeal shock wave.

Abundant data have previously shown that ischemia/infarction promptly elicits a rigorous inflammatory reaction and oxidative stress that, in turn, cause cellular apoptosis, cellular death and ultimate organ damage and dysfunction [4, 17-20, 22-24]. Another important finding in the present study was that the inflammatory reaction, oxidative stress and mitochondrial damage were substantially higher in CHP animals than SC animals. Our findings, in addition to strengthening the findings of previous studies [4, 17-20, 22-24], may also explain why fibrotic, apoptotic, DNA-damage and brain edema (i.e., AQP4) biomarkers within brain tissues were increased in the CHP group than in the SC group. These molecular-cellular perturbations were markedly suppressed in CHP animals after ECSW therapy. Our previous study showed that ECSW therapy significantly attenuated inflammation, the generation of oxidative stress, and cellular apoptosis/death in rats after acute ischaemic stroke, leading to improved neurological function and reduced brain infarct area [19]. In this way, our current findings complement those of our previous study [19], and provide an important clinically relevant indication that ECSW may be a viable alternative therapeutic option for protecting neurons from CHP-induced apoptosis/death.

Links between ischemia and organ dysfunction have been keenly investigated [4, 17-22, 24, 25]. A principal finding in the present study was that the cellular and molecular expressions of angiogenesis biomarkers, as well as small vessel density, were markedly attenuated in CHP animals compared to SC animals. Given these previous results [4, 17-22, 24, 25], our findings, at least in part, may explain why neurons, myelin sheath and mitochondria were markedly damaged in CHP animals. Of particular importance was that angiogenesis biomarkers and number of small vessels were significantly enhanced in CHP animals after ECSW therapy. Studies have previously established that the fundamental mechanisms underlying improvement of ischemia-related organ dysfunction by ECSW involve inhibition of inflammation and enhancement of angiogenesis [17-21]. Additionally, other studies have identified that restoration of blood flow by means of stem cell or ECSW therapy can protect organs from ischemia-related dysfunction [4, 17-22, 24]. In this way, our current findings support and reinforce the conclusions of previous reports [4, 17-22, 24].

Study limitations

This study has limitations. First, any behavioral changes in the rats were not assessed for. Second, WML was measured only with IHC staining but without confirmatory support by brain magnetic resonance imaging findings.

In conclusion, the results of the present study support that ECSW therapy may be an alternative option for preventing CHP-induced brain damage, which is a strong risk factor for development of ischemia-induced dementia.

Acknowledgements

This study was supported by a program grant from Chang Gung Memorial Hospital, Chang Gung University (Grant number: CMRPG8E06-81).

Disclosure of conflict of interest

None.

Address correspondence to: Dr. Hon-Kan Yip, Division of Cardiology, Department of Internal Medicine, Kaohsiung Chang Gung Memorial Hospital, 123, Dapi Road, Niaosung Dist., Kaohsiung 83301, Taiwan, R.O.C. Tel: +886-7-7317123; Fax: +886-7-7322402; E-mail: han.gung@msa.hinet.net; Sheung-Fat Ko, Department of Radiology, Kaohsiung Chang Gung Memorial Hospital, 123, Dapi Road, Niaosung Dist., Kaohsiung 83301, Taiwan, R.O.C. Tel: +886-7-7317123; Fax: +886-7-7322402; E-mail: sfatko@adm.cgmh.org.tw

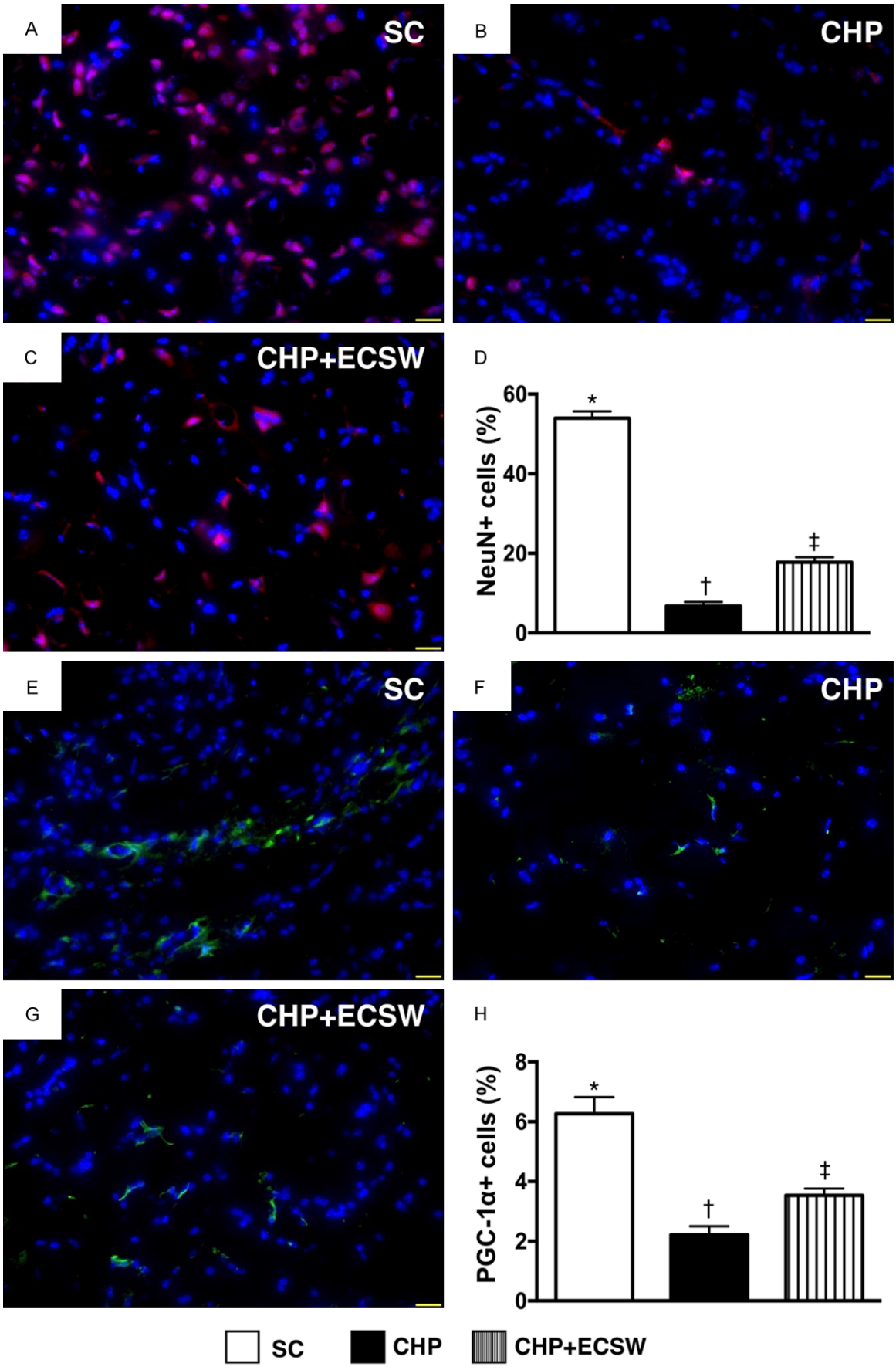
A
SC
B
CHP
C
CHP+ECSW
D
NeuN+ cells (%)
60
40
20
0
*
†
‡
E
SC
F
CHP
G
CHP+ECSW
H
PGC-1α+ cells (%)
8
6
4
2
0
*
†
‡
SC
CHP
CHP+ECSW

Figure 10. Cellular expressions of neuron and energy integrity biomarkers at day 60 after CHP induction. A-C. Illustrating microscopy findings (400×) using immunofluorescent (IF) staining to identify NeuN+ cells (red). D. Analytical result of number of positively-stained NeuN cells, * vs. other groups with different symbols (†, ‡), P<0.001. E-G. Illustrating microscopy findings (400×) using immunofluorescent (IF) staining to identify peroxisome proliferator-activated receptor-γ coactivator (PGC)-1α+ cells (green). H. Analytical result of number of positively-stained PGC-1α cells, * vs. other groups with different symbols (†, ‡), P<0.0001. Scale bars in the right lower corner represent 20 μm. All statistical analyses were performed by one-way ANOVA, followed by Bonferroni multiple comparison post hoc test (n=6). Symbols (*, †, ‡) indicate significance (at 0.05 level). SC = sham control; CHP = chronic cerebral hypoperfusion; ECSW = extracorporeal shock wave.

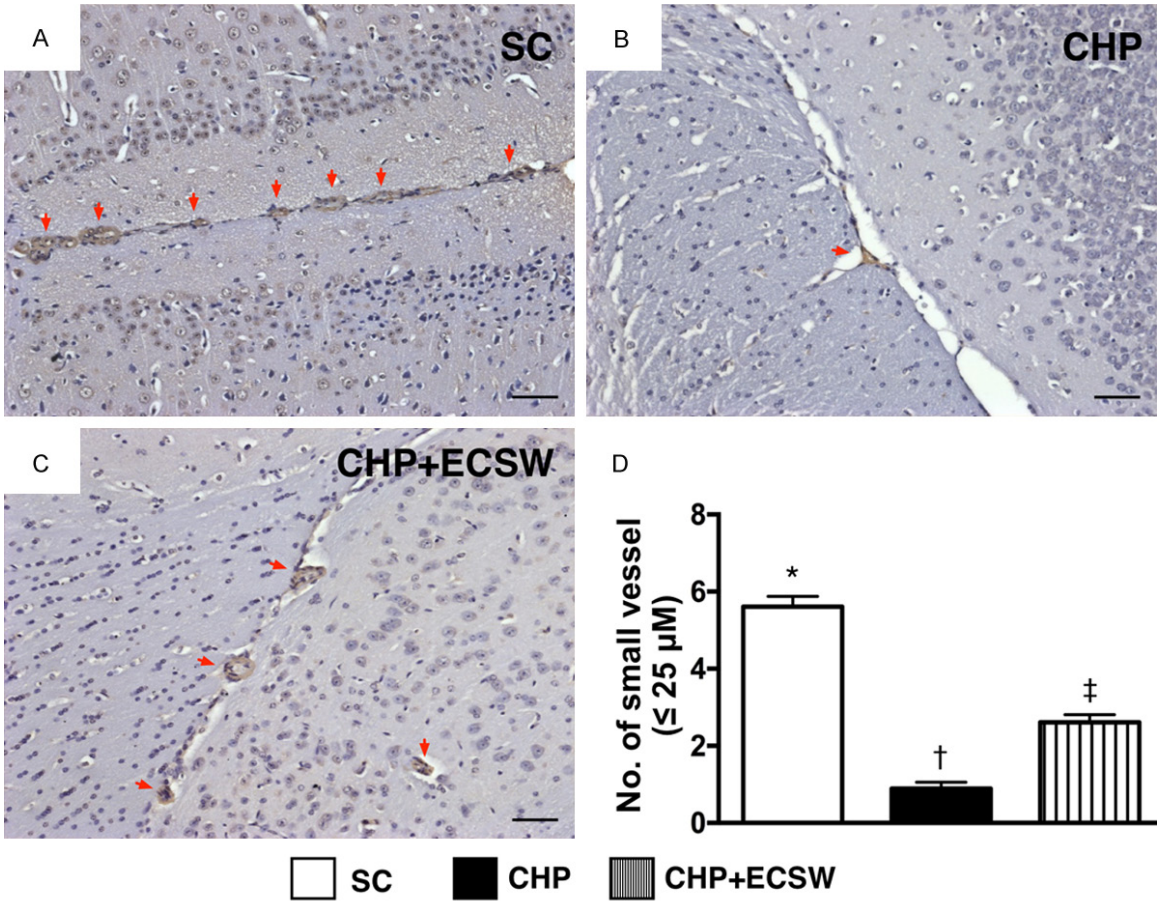

Figure 11. Small vessel (≤25 μM) density in brain tissue at day 60 after CHP induction. A-C. Illustrating microscopy (200×) for α-smooth muscle actin (α-SMA) staining to identify small vessel (red arrows) distribution in brain tissue. D. Analytical result of number of positively α-SMA stained vessels with diameter ≤25 μM, * vs. other groups with different symbols (†, ‡), P<0.0001. Scale bars in the right lower corner represent 50 μm. All statistical analyses were performed by one-way ANOVA, followed by Bonferroni multiple comparison post hoc test (n=6). Symbols (*, †, ‡) indicate significance (at 0.05 level). SC = sham control; CHP = chronic cerebral hypoperfusion; ECSW = extracorporeal shock wave.

References

[1] Mascalchi M, Ginestroni A, Toschi N, Poggesi A, Cecchi P, Salvadori E, Tessa C, Cosottini M, De Stefano N, Pracucci G, Pantoni L, Inzitari D, Diciotti S; VMCI Tuscany Investigators. The burden of microstructural damage modulates cortical activation in elderly subjects with MCI and leuko-araiosis. A DTI and fMRI study. Hum Brain Mapp 2014; 35: 819-830.

[2] Hachinski VC, Potter P and Merskey H. Leuko-araiosis. Arch Neurol 1987; 44: 21-23.

[3] Steingart A, Hachinski VC, Lau C, Fox AJ, Fox H, Lee D, Inzitari D and Merskey H. Cognitive and neurologic findings in demented patients with diffuse white matter lucencies on computed

tomographic scan (leuko-araiosis). Arch Neurol 1987; 44: 36-39.
[4] Tsai TH, Sun CK, Su CH, Sung PH, Chua S, Zhen YY, Leu S, Chang HW, Yang JL and Yip HK. Sitagliptin attenuated brain damage and cognitive impairment in mice with chronic cerebral hypo-perfusion through suppressing oxidative stress and inflammatory reaction. J Hypertens 2015; 33: 1001-1013.
[5] Roman GC, Erkinjuntti T, Wallin A, Pantoni L and Chui HC. Subcortical ischaemic vascular dementia. Lancet Neurol 2002; 1: 426-436.
[6] Gorelick PB and Pantoni L. Advances in vascular cognitive impairment. Stroke 2013; 44: 307-308.
[7] Rincon F and Wright CB. Vascular cognitive impairment. Curr Opin Neurol 2013; 26: 29-36.
[8] Scherr M, Trinka E, Mc Coy M, Krenn Y, Staffen W, Kirschner M, Bergmann HJ and Mutzenbach JS. Cerebral hypoperfusion during carotid artery stenosis can lead to cognitive deficits that may be independent of white matter lesion load. Curr Neurovasc Res 2012; 9: 193-199.
[9] Gill R, Tsung A and Billiar T. Linking oxidative stress to inflammation: toll-like receptors. Free Radic Biol Med 2010; 48: 1121-1132.
[10] Zhang W, Smith C, Howlett C and Stanimirovic D. Inflammatory activation of human brain endothelial cells by hypoxic astrocytes in vitro is mediated by IL-1beta. J Cereb Blood Flow Metab 2000; 20: 967-978.
[11] Choi BR, Lee SR, Han JS, Woo SK, Kim KM, Choi DH, Kwon KJ, Han SH, Shin CY, Lee J, Chung CS, Lee SR and Kim HY. Synergistic memory impairment through the interaction of chronic cerebral hypoperfusion and amlyloid toxicity in a rat model. Stroke 2011; 42: 2595-2604.
[12] Tomimoto H, Ihara M, Wakita H, Ohtani R, Lin JX, Akiguchi I, Kinoshita M and Shibasaki H. Chronic cerebral hypoperfusion induces white matter lesions and loss of oligodendroglia with DNA fragmentation in the rat. Acta Neuropathol 2003; 106: 527-534.
[13] Ueno M, Tomimoto H, Akiguchi I, Wakita H and Sakamoto H. Blood-brain barrier disruption in white matter lesions in a rat model of chronic cerebral hypoperfusion. J Cereb Blood Flow Metab 2002; 22: 97-104.
[14] Wakita H, Tomimoto H, Akiguchi I and Kimura J. Glial activation and white matter changes in the rat brain induced by chronic cerebral hypoperfusion: an immunohistochemical study. Acta Neuropathol 1994; 87: 484-492.
[15] Ma HZ, Zeng BF and Li XL. Upregulation of VEGF in subchondral bone of necrotic femoral heads in rabbits with use of extracorporeal shock waves. Calcif Tissue Int 2007; 81: 124-131.
[16] Wang CJ, Wang FS, Yang KD, Weng LH, Hsu CC, Huang CS and Yang LC. Shock wave therapy induces neovascularization at the tendon-bone junction. A study in rabbits. J Orthop Res 2003; 21: 984-989.
[17] Fu M, Sun CK, Lin YC, Wang CJ, Wu CJ, Ko SF, Chua S, Sheu JJ, Chiang CH, Shao PL, Leu S and Yip HK. Extracorporeal shock wave therapy reverses ischemia-related left ventricular dysfunction and remodeling: molecular-cellular and functional assessment. PLoS One 2011; 6: e24342.
[18] Yeh KH, Sheu JJ, Lin YC, Sun CK, Chang LT, Kao YH, Yen CH, Shao PL, Tsai TH, Chen YL, Chua S, Leu S and Yip HK. Benefit of combined extracorporeal shock wave and bone marrow-derived endothelial progenitor cells in protection against critical limb ischemia in rats. Crit Care Med 2012; 40: 169-177.
[19] Yuen CM, Chung SY, Tsai TH, Sung PH, Huang TH, Chen YL, Chen YL, Chai HT, Zhen YY, Chang MW, Wang CJ, Chang HW, Sun CK and Yip HK. Extracorporeal shock wave effectively attenuates brain infarct volume and improves neurological function in rat after acute ischemic stroke. Am J Transl Res 2015; 7: 976-994.
[20] Sheu JJ, Lee FY, Yuen CM, Chen YL, Huang TH, Chua S, Chen YL, Chen CH, Chai HT, Sung PH, Chang HW, Sun CK and Yip HK. Combined therapy with shock wave and autologous bone marrow-derived mesenchymal stem cells alleviates left ventricular dysfunction and remodeling through inhibiting inflammatory stimuli, oxidative stress & enhancing angiogenesis in a swine myocardial infarction model. Int J Cardiol 2015; 193: 69-83.
[21] Nishida T, Shimokawa H, Oi K, Tatewaki H, Uwatoku T, Abe K, Matsumoto Y, Kajihara N, Eto M, Matsuda T, Yasui H, Takeshita A and Sunagawa K. Extracorporeal cardiac shock wave therapy markedly ameliorates ischemia-induced myocardial dysfunction in pigs in vivo. Circulation 2004; 110: 3055-3061.
[22] Chen YL, Tsai TH, Wallace CG, Chen YL, Huang TH, Sung PH, Yuen CM, Sun CK, Lin KC, Chai HT, Sheu JJ, Lee FY and Yip HK. Intra-carotid arterial administration of autologous peripheral blood-derived endothelial progenitor cells improves acute ischemic stroke neurological outcomes in rats. Int J Cardiol 2015; 201: 668-683.
[23] Yip HK, Yuen CM, Chen KH, Chai HT, Chung SY, Tong MS, Chen SY, Kao GS, Chen CH, Chen YL, Huang TH, Sun CK and Lee MS. Tissue plasminogen activator deficiency preserves neurological function and protects against murine acute ischemic stroke. Int J Cardiol 2016; 205: 133-141.
[24] Chen KH, Chen CH, Wallace CG, Yuen CM, Kao GS, Chen YL, Shao PL, Chen YL, Chai HT, Lin

KC, Liu CF, Chang HW, Lee MS and Yip HK. Intravenous administration of xenogenic adipose-derived mesenchymal stem cells (ADMSC) and ADMSC-derived exosomes markedly reduced brain infarct volume and preserved neurological function in rat after acute ischemic stroke. Oncotarget 2016; 7: 74537-74556.

[25] Shibata M, Ohtani R, Ihara M and Tomimoto H. White matter lesions and glial activation in a novel mouse model of chronic cerebral hypoperfusion. Stroke 2004; 35: 2598-2603.